



Knockdown of Two Iodothyronine Deiodinase Genes Inhibits Epinephrine-Induced Larval Metamorphosis of the Hard-Shelled Mussel *Mytilus coruscus*

Xue Shi^{1,2†}, Yu-Qing Wang^{1,2†}, Yue-Ming Yang^{1,2} and Yi-Feng Li^{1,2*}

¹International Research Center for Marine Biosciences, Ministry of Science and Technology, Shanghai Ocean University, Shanghai, China, ²Key Laboratory of Exploration and Utilization of Aquatic Genetic Resources, Ministry of Education, Shanghai Ocean University, Shanghai, China

OPEN ACCESS

Edited by:

Valerio Matozzo,
University of Padua, Italy

Reviewed by:

Huihui Liu,
Zhejiang Ocean University,
China;
Andrew Gracey,
University of Southern California,
United States

*Correspondence:

Yi-Feng Li
yifengli@shou.edu.cn

[†]These authors have contributed
equally to this work

Specialty section:

This article was submitted to
Aquatic Physiology,
a section of the journal
Frontiers in Marine Science

Received: 06 April 2022

Accepted: 06 June 2022

Published: 14 July 2022

Citation:

Shi X, Wang Y-Q, Yang Y-M
and Li Y-F (2022) Knockdown of Two
Iodothyronine Deiodinase Genes
Inhibits Epinephrine-Induced Larval
Metamorphosis of the Hard-Shelled
Mussel *Mytilus coruscus*.
Front. Mar. Sci. 9:914283.
doi: 10.3389/fmars.2022.914283

The metamorphosis process is a critical life-changing event for marine invertebrate planktonic larvae to transform into benthic adults, which is crucial for the shellfish bed's ecosystem stability and seed production in aquaculture. The mechanism of neuroendocrine regulation in the larval metamorphosis of bivalves remains ambiguous. In the present study, the expression of two deiodinase genes, *McDx* and *McDy*, was analyzed by whole-mount *in situ* hybridization at four larval stages in the hard-shelled mussel *Mytilus coruscus*. The *McDx* and *McDy* localized in visceral tissues, nervous system, mantle, and velum, indicating that two deiodinase genes are essential for larval development in *M. coruscus*. Knockdown of the *McDx* and *McDy* in the pediveliger larvae of *M. coruscus* using electroporation of siRNA significantly ($p < 0.001$) reduced *McDx* and *McDy* expression. *McDx* and *McDy* knockdown reduced larval metamorphosis in 45% and 49% of the pediveliger larvae induced by epinephrine (EPI). It is hypothesized that the knockdown effects of *McDx* and *McDy* repress metamorphic induction rather than larval viability, which does not elicit a lethal effect. The present study corroborates a synergistic action of the adrenergic and thyroid hormones signalling pathway in *M. coruscus*, and suggests the role of *McDx* and *McDy* in larval development and metamorphic transition.

Keywords: larval metamorphosis, *Mytilus coruscus*, iodothyronine deiodinase, electroporation, siRNA transfection

INTRODUCTION

Most marine invertebrates have a biphasic life cycle encompassing planktonic larva and sessile adult phases (Burke, 1983). Larvae spend varying amounts of time enabling themselves to become competent to respond to the biotic and abiotic inducers and metamorphose into an adult form (Qian, 1999; Hadfield, 2000). Metamorphosis is accompanied by spectacular morphological and physiological changes, including remodeling tissue structures (Strathmann, 1978). This metamorphic transition is correlated with the irreversible loss of larval structures and the acquisition of juvenile tissues (Li et al., 2020). Larvae of marine invertebrates detect chemical cues from marine biofilms exogenously and translate environmental cues internally to activate metamorphosis processes via neuronal and hormonal elements (Hadfield, 2011). Neuroendocrine signalling is involved in various marine invertebrates across metamorphic development, given that the chemical inducers efficiently

promote larval metamorphosis in bivalve aquaculture (Joyce and Vogeler, 2018).

In vertebrates, the thyroid hormones (THs) signalling pathway is crucial for the larva to juvenile transformation (Power et al., 2001; Paris and Laudet, 2008). Work on metamorphosis in anurans and teleost has clearly revealed the up-regulation of THs signalling elements during metamorphosis (Laudet, 2011). Three types of iodothyronine deiodinases, type 1 (D1), type 2 (D2), and type 3 (D3), are enzymes that are essential for activating and deactivating the THs molecules to increase or decrease activity (Darras and Van Herck, 2012). The importance of deiodinases in mediating TH-driven tissue morphogenesis is exemplified in teleost and anuran metamorphosis. The increased expression of D1 and D2 was positively correlated with the metamorphic changes in Atlantic halibut *Hippoglossus hippoglossus* and sea bream *Sparus aurata* (Campinho et al., 2010; Campinho et al., 2012). D2 has been reported as a crucial TH-signalling mediator gene for the asymmetric development during flatfish metamorphosis (Campinho et al., 2018). Exposure to deiodinase inhibitor propylthiouracil (PTU) represses the limbs development of *Xenopus tropicalis* (Carlsson and Norrgren, 2007).

Homologues of the vertebrate deiodinases have been found in some invertebrate species. An iodothyronine deiodinase gene with outer-ring deiodinase activity has been identified in ascidian *Halocynthia roretzi* (Shepherdley et al., 2004). In a mollusc, two deiodinases were identified in the Pacific oyster *Crassostrea gigas*, and increased expression of two deiodinase genes was promoted by epinephrine (Huang et al., 2015). Epinephrine is a potent chemical inducer for promoting larval metamorphosis in many bivalve species, including oysters and mussels (Joyce and Vogeler, 2018). Previously we identified two deiodinase genes (*McDx* and *McDy*) in the mussel *Mytilus coruscus* (Li et al., 2021), and the potential role in larval metamorphosis remains unknown.

A thyroid hormone receptor (*McTR*) gene was identified in *M. coruscus*, and knockdown of *McTR* reduced larval metamorphosis in response to the metamorphosis inducer epinephrine (Li et al., 2020). Moreover, THs synthesis and metabolism inhibitor compounds methimazole (MMI) and PTU significantly reduced larval metamorphosis induced by epinephrine in *M. coruscus* (Li et al., 2021). The obtained results led us to hypothesize that crosstalk between adrenergic and THs signalling pathways can occur. We analyzed the expression pattern of *McDx* and *McDy* in four larval stages using whole-mount *in situ* hybridization (WISH). To further understand that *McDx* and *McDy* can regulate larval metamorphosis, we used the *McDx* and *McDy* knockdown approach by siRNA transfection by electroporation and was evaluated by quantitative real-time PCR (qPCR). Knockdown of *McDx* and *McDy* reduced larval metamorphosis in 45% and 49% ($p < 0.001$) of the pediveliger larvae that had been induced by epinephrine.

MATERIAL AND METHODS

M. coruscus Larval Culture and Sampling

Adult *M. coruscus* were collected from Gouqi island (30°72'N; 122°77'E), Zhoushan, Zhejiang Province, China. Spawning and

larvae culture methods were performed as previously described (Li et al., 2020). Adult mussels were washed in seawater (salinity: 30 ppt) and induced for spawning by ice shock. Mussels that started spawning were transferred to 2L glass beakers. Fertilization was carried out by gently mixing eggs and sperms in filtered seawater (FSW; acetate-fibre filter: 1.2 µm pore size). The excess sperms were filtered through a nylon plankton net (mesh size: 20 µm) and kept them undisturbed in FSW at 18°C for two days. The seawater was renewed every other day. Larvae were fed with microalgae *Isochrysis zhanjiangensis* and maintained at a density of 5 larvae mL⁻¹ at 18°C. Larvae samples were collected at 1 dpf (trochophore larvae), 2 dpf (D-veliger larvae), 15 dpf (umbo larvae) and 41 dpf (pediveliger larvae) and relaxed with 1M MgCl₂ in FSW, then collected into ice-cold 4% PFA/1×PBS (pH 7.4) for 2h. Samples were replaced with fresh 4% PFA/1×PBS and kept at 4°C overnight. Samples were washed in 1×PBS + 0.1% Tween 20 (PBT) and progressively dehydrated with methanol (MeOH)/PBT (100% MeOH to 0% MeOH) and transferred to 100% MeOH and stored at -20°C for whole-mount *in situ* hybridization (WISH) and whole-mount immunohistochemistry (IHC). The experimental tests and animal handling procedures performed in this study were approved by the Institutional Animal Care and Use Committee (IACUC) of Shanghai Ocean University with the registration number of SHOU-DW-2018-013.

Whole-Mount *In Situ* Hybridization

Fragments of 365 bp of *McDx* (Accession number: MW928628) and 384 bp of *McDy* (Accession number: MW928627) genes were amplified from larval cDNA using gene-specific primers containing a T7 promoter sequence (5'-TAATACGACTCACTATAGGG-3'). A T7 RNA polymerase promoter was added in the reverse primer (for antisense probe) or forward primer (for sense probe) for amplifying the probe template. Digoxigenin-labeled sense and anti-sense riboprobes were synthesized by *in vitro* transcription using purified polymerase chain reaction products as templates using MAXIscript™ T7 (Thermo Fisher, USA) and DIG RNA labeling Mix (Roche), and stored at -80°C. Hybridization with sense riboprobes was conducted as a negative control in the assay.

For the WISH, all steps were performed at room temperature unless otherwise indicated. Larvae samples in 100% MeOH were gradually hydrated by continuous washing in MeOH/PBT (100% MeOH to 0% MeOH) for 5 min. Samples were digested with proteinase K (20 µg mL⁻¹) in PBT and hybridized with 0.5-1 µg mL⁻¹ DIG-labeled cRNA probe at 65°C overnight. Specimens were stained with 1/5000 anti-digoxigenin antibody conjugated to alkaline phosphatase (Roche) overnight at 4°C. Samples were washed in PBT and then incubated in NBT (nitro blue tetrazolium)/BCIP (5-Bromo-4-chloro-3-indolylphosphate, Roche) for color development in the dark and washed in PBT to stop the reaction. Images were captured with a Zeiss Axio Imager M2 microscope coupled to an axiocam 305 digital camera.

Whole-Mount Immunohistochemistry

Larvae samples in 100% MeOH were hydrated as described above and washed with 1×PBS. Hydrated samples were decalcified

with 5% EDTA in PBS for 30 min at room temperature and then preincubated with blocking solution (0.25% BSA+0.03% NaN₃+1% Triton X-100+1×PBS) at 4°C for 2-4 h to eliminate non-specific binding sites. The specimens were then washed in 1×PBS+1% Triton X-100 (PBTr) and incubated with primary antibodies at a final dilution of 1:1000 in the blocking solution for 2 days at 4°C using a polyclonal antibodies against FMRFamide or 5-HT (Immunostar, Hudson, WI, USA). Fluorescently tagged AlexaFluor 488 goat anti-rabbit IgG (sigma, USA) was used to detect the primary antisera. After the whole mount-staining, pediveliger larvae were washed with PBTr and stored in 100% glycerol for image acquisition using a Leica TCS SP8 confocal laser scanning microscopes.

siRNA Synthesis

The siRNA probe for *McDx*, nucleotides 240-258 across the open reading frame (ORF; **Supplementary Figure 1**), and siRNA probe against *McDy*, spanned nucleotides 549-567 across the ORF (**Supplementary Figure 2**). The siRNA oligonucleotide sequences specific to *McDx* (5'-ccaauacgguagagaaau-3') or *McDy* (5'-gccuuuauugguuagcuu-3') were confirmed by BLAST search of an in-house *M. coruscus* transcriptome database. The double-stranded siRNA was synthesized by GenePharma Co. Ltd. (Shanghai, China). The non-sense siRNA (5'-uucuccgaacgugucacgu-3') was not annealed to non-target gene transcripts of *M. coruscus* transcriptome database (Li et al., 2020).

siRNA Transfection by Electroporation

siRNA transfection in pediveliger larvae of *M. coruscus* was conducted following the method described previously (Li et al., 2020). In summary, the pooled pediveliger larvae were transferred to 1.5-ml tubes containing 1 ml autoclaved filtered seawater (AFSW) and 0.4 or 0.8 µg target or NC siRNA. An untreated control group without adding siRNA was set up following the same procedure for transfection.

The siRNA/larvae electroporation was carried out in Gene Pulser Xcell (Bio-Rad, USA) with square-wave pulses in a 0.4 cm electroporation cuvette. The electroporation protocol was used as follows: one pulse of 100 V was administered for 5 ms, followed immediately by 10 pulses of 50 V for 20 ms (with a 1 s interval between pulses). After electroporation, the siRNA-larva

mixture was left undisturbed at room temperature for 10 minutes and then transferred to 10 L polycarbonate tanks (containing 5 L AFSW at 20°C). 1440 electroporated larvae were maintained in 5 L AFSW for 24 h prior to larval metamorphic bioassays. The larvae electroporated with siRNA (Dx, Dy or NC) or without siRNA (control, C) were used for qPCR analysis and were cultured for 48 hours without feeding prior to sampling. The experimental set-up is shown in **Table 1**.

Larval Metamorphosis

Larval metamorphosis bioassays were carried out according to the methods described previously (Yang et al., 2014; Li et al., 2020). Epinephrine (EPI) was used as a strong inducer for larval metamorphosis based on previous results in *M. coruscus* (Yang et al., 2014; Li et al., 2020). 1440 electroporated larvae were used for the metamorphosis bioassays. Nine replicates of each experimental treatment group were carried out. Treated larvae were transferred into Petri dishes (Ø 60 mm × 19 mm height) containing 20 pediveliger larvae and 20 mL test solution (10⁻⁴ M EPI) for 96 h. The EPI test solution was not changed during the exposure. Blank control (BC) was incubated in 20 mL AFSW by twenty larvae without electroporation or exposure to EPI. The maximum metamorphosis rate was determined using pediveliger larvae exposed to 10⁻⁴ M EPI, which was set up as a positive control (PC). All assays were conducted in a dark environment at 18 ± 1°C. The larvae of each treatment group were observed daily under an Olympus stereoscopic microscope, and the dead larvae were removed and counted. Post-larvae lost their velum and exhibited post-larval shell growth (Li et al., 2020).

Total RNA Extraction

Total RNA was extracted from five independent larval pools of treatment groups using RNAiso Plus reagent following the manufacturer's protocol (Takara, Japan) and genomic DNA was removed by a PrimeScript™ RT kit with gDNA eraser (Takara, Japan) and cDNA synthesis was performed using the PrimeScript Reagent Kit (Takara, Japan) with DNase-treated RNA.

Quantitative Real-Time PCR Analysis

Quantitative real-time PCR (qPCR) reaction was performed duplicate and each reaction containing 1 µL template cDNA, 0.3 µL of each forward and reverse primers (10 mM, **Table 2**), 5 µL of 2 × FastStart Essential DNA Green Master (Roche) and

TABLE 1 | The experimental set-up.

	siRNA (µg)	Electroporation	EPI (10 ⁻⁴ M)	qPCR	Survival bioassays
Blank control (BC)	0	–	–	–	√
Positive control (PC)	0	√	√	–	√
Control (C)	0	√	–	√	–
Negative control siRNA (NC siRNA)	0.4	√	√	√	√
Negative control siRNA (NC siRNA)	0.8	√	√	√	√
Dx-siRNA	0.4	√	√	√	√
Dx-siRNA	0.8	√	√	√	√
Dy-siRNA	0.4	√	√	√	√
Dy-siRNA	0.8	√	√	√	√

The symbol “√” indicates the experimental treatment administered. BC was not subject to electroporation or treated with EPI. PC was electroporated and treated with EPI. C was electroporated but not treated with EPI. NC siRNA, Dx-siRNA and Dy-siRNA were electroporated with siRNA and treated with EPI.

sigma water to give a final reaction volume of 10 μL . All samples were carried out in 96 multi-well plates using a LightCycler 960 (Roche) with five biological replicates and two technical replicates per sample were carried out. Gene expression was determined by the absolute quantification method using gel isolated amplicons as standards as previously described (Li et al., 2021). The qPCR amplification protocol was carried out as follows: the initial denaturation step for 10 min at 95°C, followed by 45 cycles of 10 s at 95°C and 10 s at 60°C. A melting curve analysis confirmed that a single reaction peak was obtained in the qPCR reaction.

Statistical Analysis

Data were analysed for statistical difference by using JMP™ software. $p < 0.05$ was the cut-off for statistical difference. The percentage of post-larvae (metamorphosis data) was arcsine-transformed and then tested for normality and homogeneity. A Wilcoxon/Kruskal Wallis test was used to assess the gene expression and larval metamorphosis data.

RESULTS

WISH Analysis of *McDx* and *McDy* During Ontogeny

Transcripts localization of *McDx* and *McDy* was examined by WISH in four developmental larval stages (trochophore, D-veliger, umbo and pediveliger larvae) (Figure 1). At the trochophore larvae stage, the expression of *McDx* and *McDy* was both detected in telotroch and prototroch (Figures 1A, E; Supplementary Figure 3A). The *McDx* was also expressed in the central region of the shell field of the larva (Figure 1A). In the stage of the D-veliger larvae, the expression of *McDx* and *McDy* was mainly expressed in the mantle region (located at the edge of the shell) (Figures 1B, F). At the umbo larvae stage, *McDx* and *McDy* transcripts were detected in the visceral tissues region (Figures 1C, G). In the pediveliger larvae stage, the distinct expression patterns of *McDx* and *McDy* transcripts were observed, showing the functional differentiation among two deiodinase genes (Figures 1D, H). *McDx* was extensively expressed in the visceral tissues and medial region originating from the apical to the caudal region of the pediveliger larvae (Figure 1D). The expression of *McDy* was found in the edge of the velum (the organ responsible for motor and feeding functions) and mantle region correlated with shell development (Figure 1H; Supplementary Figure 3B).

Immunohistochemical Analysis of *McDx* and *McDy* During Ontogeny

To understand the *McDx* signal localized in the median body region of pediveliger larvae, IHC with the antibodies against FMRFamide and 5-HT, markers for the ganglia and developing nervous system, were conducted to visualize the neural development (Figure 2). The FMRFamide immunoreactive (FMRFamide-ir) cell appeared at three pairs of ganglia (cerebral, pedal and visceral) and interconnecting connectives and commissures (Figures 2A, B). The 5-HT-like immunoreactive (5-HT-*lir*) cells were detected in the cerebral ganglia and were seen to innervate the velum and ventral part of the body, including the mantel area and regions of the pedal and visceral ganglia (Figures 2C, D). The expression of *McDx* in the median body region of pediveliger larvae likely corresponds to the position of 5-HT-*lir* neurons (Figures 1D, 2C, D).

McDx and *McDy* Involved in Larval Metamorphosis

The expression of *McDx* and *McDy* were significantly reduced in electroporated pediveliger larvae exposed to 0.4 $\mu\text{g mL}^{-1}$ and 0.8 $\mu\text{g mL}^{-1}$ *McDx* siRNA or *McDy* siRNA (0.4 *McDx* and 0.8 *McDx*; 0.4 *McDy* and 0.8 *McDy*) compared to the control group (C) and the non-sense siRNA negative controls (0.4 NC and 0.8 NC, $p < 0.05$, Figures 3A, 4A). In contrast, there was no significant difference between the non-sense siRNA negative controls and the control group ($p > 0.05$, Figures 3A, 4A).

No metamorphosis occurred in the electroporation larvae that were not exposed to siRNA and treated with EPI (BC, Figures 3B, 4B). 44% of pediveliger larvae underwent metamorphosis induced by EPI after electroporation without siRNA (PC, Figures 3B, 4B). Electroporation of pediveliger larvae using 0.8 $\mu\text{g mL}^{-1}$ *McDx* siRNA significantly reduced larval metamorphosis after 96 h of EPI exposure relative to 0.8 $\mu\text{g mL}^{-1}$ non-sense siRNA electroporation and the PC group ($p < 0.05$, Figure 3B). Larval metamorphosis was significantly inhibited in electroporated pediveliger larvae using 0.4 $\mu\text{g mL}^{-1}$ and 0.8 $\mu\text{g mL}^{-1}$ *McDy* compared to 0.4 $\mu\text{g mL}^{-1}$ and 0.8 $\mu\text{g mL}^{-1}$ of NC groups, respectively ($p < 0.05$, Figure 4B).

Metamorphosed post-larvae were firstly found in 48 h after being treated with EPI, and the number of post-larvae increased gradually with increasing exposure time to 96 h (Figures 3C, 4C). The electroporation of 0.4 $\mu\text{g mL}^{-1}$ and 0.8 $\mu\text{g mL}^{-1}$ *McDx* siRNA significantly reduced the larval metamorphosis rate by 32% ($p < 0.05$) and 45% ($p < 0.001$) compared to the PC group, respectively

TABLE 2 | List of the primers used in real-time quantitative PCR (RT-qPCR) in this study.

Primer	Sequence (5'-3')	Amplicon Size (bp)	r ²	Efficiency (%)	Application
Dx-F	AGCTGCTCTTGACCAACCGTTTATG	142	0.99	100	RT-qPCR
Dx-R	ACGTTGTGCCTTGTACACTCCATTC				RT-qPCR
Dy-F	TTCAAACAAGTATGGAGGGCGATGT	179	0.99	90	RT-qPCR
Dy-R	AACGGCCGGTCACGAACAACCTG				RT-qPCR
EF-1 α -F	CACCACGAGTCTCTCCCTGA	105	0.99	95	RT-qPCR
EF-1 α -R	GCTGTCAACCACAGACCAATCC				RT-qPCR

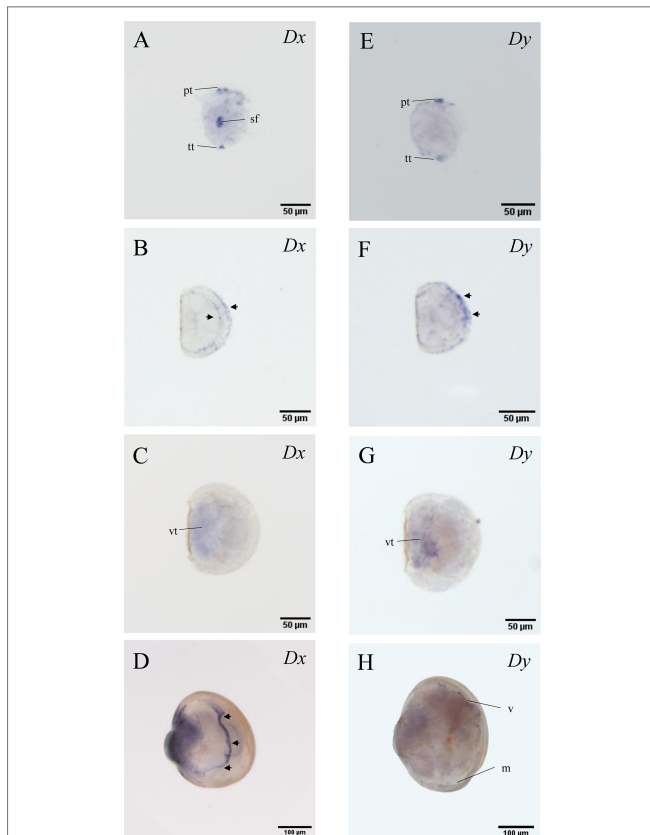


FIGURE 1 | *McDx* and *McDy* expression changes in four larval stages of *M. coruscus*. The apical pole is always upward and the ventral side is on the right except for A and E. **(A, E)** trochophore larvae (dorsal view); *McDx* and *McDy* signals in the prototroch and telotroch. *McDx* expressed in the shell field. **(B, F)** D-veliger larvae; *McDx* and *McDy* signals are located at the edge of the shell (arrow). **(C, G)** umbo larvae; *McDx* and *McDy* expressed in the visceral tissues. **(D, H)** pediveliger larvae; *McDx* expressed in the medial region originating from the apical to the caudal region of the larva (arrow). *McDy* is expressed in the edge of the velum and mantle. pt, prototroch; tt, telotroch; sf, shell field; vt, visceral tissues; v, velum; m, mantel.

(Figure 3C). The larval metamorphosis rate of exposure to 0.4 $\mu\text{g mL}^{-1}$ and 0.8 $\mu\text{g mL}^{-1}$ *McDy* siRNA significantly reduced by 38% ($p < 0.05$) and 49% ($p < 0.001$) compared to the PC group, respectively (Figure 4C). Larval viability from 48 h onwards after electroporation significantly declined ($p < 0.05$) in 0.8 $\mu\text{g mL}^{-1}$ of NC groups compared to other groups (Figure 4D).

DISCUSSION

The present study reports that two deiodinase genes are both expressed during larval development, and distinct expression patterns of *McDx* and *McDy* in the pediveliger stage reflect the functional differentiation among two deiodinase genes in *M. coruscus*. The results of IHC further revealed that *McDx* might be vital for neural development in the pediveliger larvae. It further demonstrates that knockdown of the gene expression of *McDx* and *McDy* impairs the metamorphosis process as a consequence

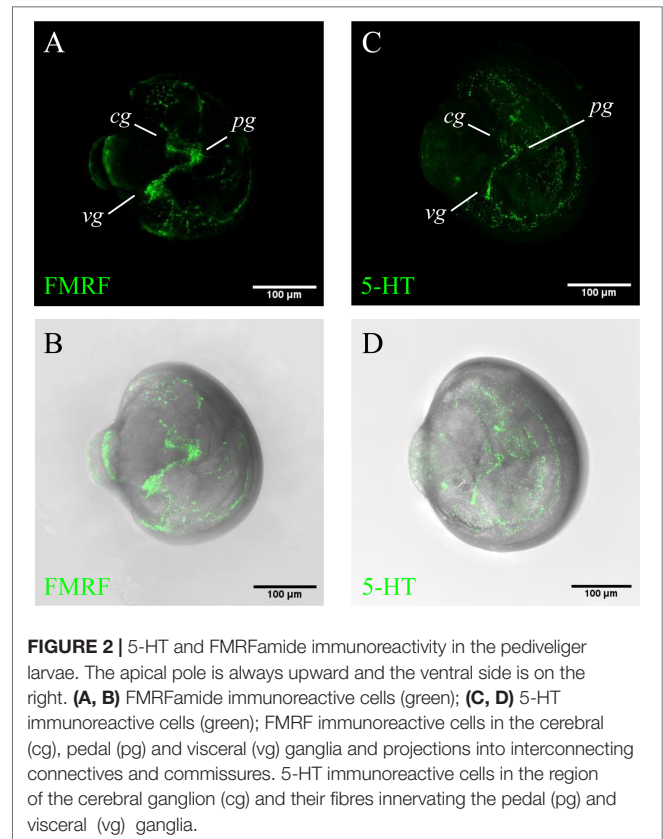


FIGURE 2 | 5-HT and FMRFamide immunoreactivity in the pediveliger larvae. The apical pole is always upward and the ventral side is on the right. **(A, B)** FMRFamide immunoreactive cells (green); **(C, D)** 5-HT immunoreactive cells (green); FMRF immunoreactive cells in the cerebral (cg), pedal (pg) and visceral (vg) ganglia and projections into interconnecting connectives and commissures. 5-HT immunoreactive cells in the region of the cerebral ganglion (cg) and their fibres innervating the pedal (pg) and visceral (vg) ganglia.

of the reduction of epinephrine-induced larval metamorphosis in *M. coruscus*.

The results of WISH revealed that the *McDx* and *McDy* had a similar expression pattern in telotroch and prototroch of the trochophore larvae and both tissues are locomotory organs with motor function, which suggests that the *McDx* and *McDy* might be involved in the development of locomotory organs (Figures 1A, E; Supplementary Figure 3A). Besides, the expression of *McDx* appeared in the shell field of the trochophore larvae (Figure 1A), which may support a role in regulating the first original shell development (Huan et al., 2020). The mantle organ, a biomineralization-related tissue of molluscs, is situated alongside the shell edge (the hinge is located in the posterior region) (Li et al., 2017). The expression of the *McDx* and *McDy* was spatially enriched in the mantle region, implicating the regulation of shell production in the D-veliger larvae (Figures 1B, F). The consistent expression pattern of the *McDx* and *McDy* in the visceral region of the umbo larvae allows us to suggest that it plays an intrinsic role in somatic tissue development (Figures 1C, G). The higher expression pattern of *McDx*, together with lower *McDy* expression in visceral mass (Figures 1D, H), suggests that two deiodinase genes are essential for the growth and development of the somatic tissue in the pediveliger larvae. Similar observations have been reported in zebrafish embryos showing abundant D1 expressed in the somatic tissues such as the liver, gut and kidney (Thisse et al., 2003). Interestingly, an exclusive stripe-like *McDx* signal originating from the apical to the caudal region appears

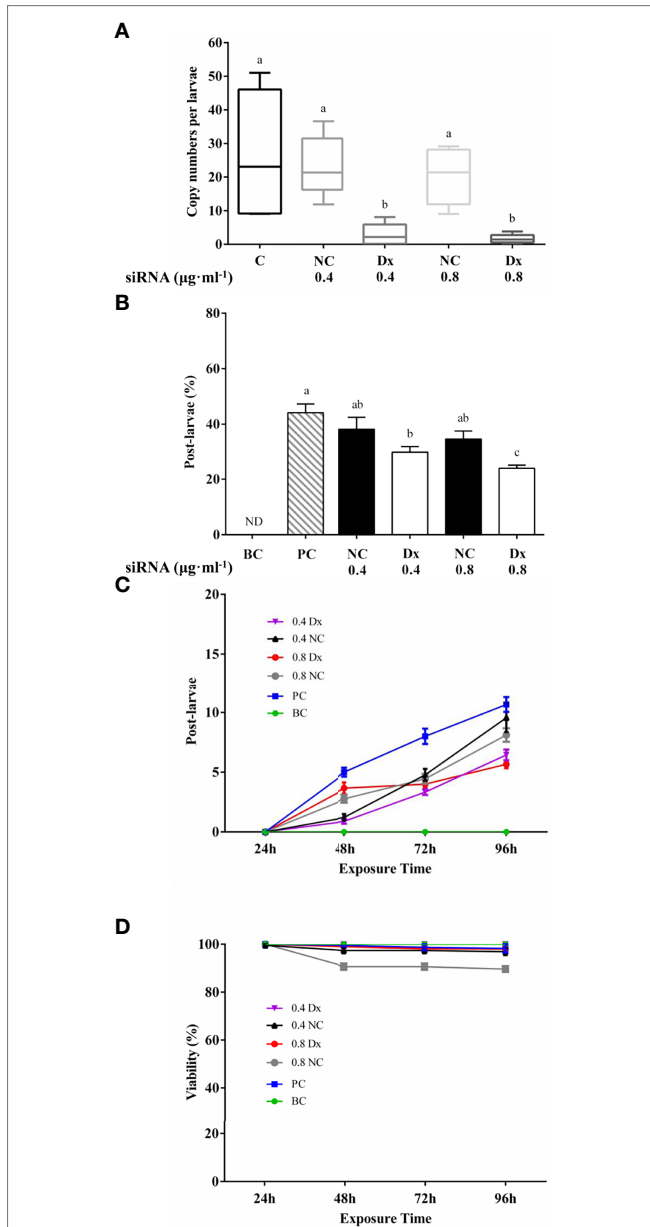


FIGURE 3 | Effect of electroporation on *McDx* expression (A), metamorphosis (B), the cumulative number of post-larvae (C) and viability (D) of the hard-shelled mussel larvae. (A) Quantitative RT-PCR expression of the *McDx* in electroporated and control larvae. Significant differences ($p < 0.05$) are represented by different letters above the columns. C: control; NC: negative control (electroporated with the non-sense siRNA, 0.4 and 0.8 µg ml⁻¹); Dx: electroporated with the *McDx* siRNA (0.4 and 0.8 µg ml⁻¹). (B) Percentage of larvae metamorphosed at 96 h. The results are represented as mean ± SEM of nine experiments containing 20 larvae per replicate. Different letters above the bars indicate statistically significant differences ($p < 0.05$). BC: blank control; PC: positive control; NC: negative control (electroporated with the non-sense siRNA, 0.4 and 0.8 µg ml⁻¹); Dx: electroporated with the *McDx* siRNA (0.4 and 0.8 µg ml⁻¹). (C) The cumulative number of post-larvae at each time point of the metamorphosis assay (EPI induction) in control and *McDx* siRNA, non-sense siRNA electroporated pediveliger larvae. The results are presented as the mean ± SEM of nine experimental replicates (each containing 20 individuals). (D) Viability of mussel larvae in the metamorphosis assay (EPI induction) after electroporation with *McDx* siRNA or non-sense siRNA.

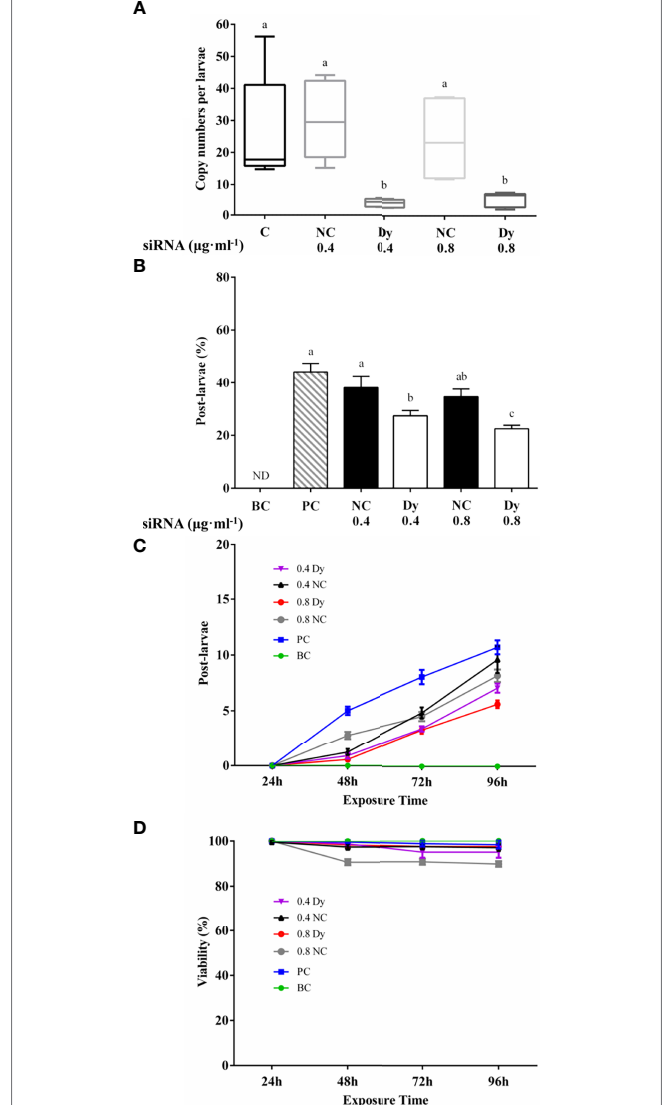


FIGURE 4 | Effect of electroporation on *McDy* expression (A), metamorphosis (B), the cumulative number of post-larvae (C) and viability (D) of the hard-shelled mussel larvae. (A) Quantitative RT-PCR expression of the *McDy* in electroporated and control larvae. Significant differences ($p < 0.05$) are represented by different letters above the columns. C: control; NC: negative control (electroporated with the non-sense siRNA, 0.4 and 0.8 µg ml⁻¹); Dy: electroporated with the *McDy* siRNA (0.4 and 0.8 µg ml⁻¹). (B) Percentage of larvae metamorphosed at 96 h. The results are represented as mean ± SEM of nine experiments containing 20 larvae per replicate. Different letters above the bars indicate statistically significant differences ($p < 0.05$). BC: blank control; PC: positive control; NC: negative control (electroporated with the non-sense siRNA, 0.4 and 0.8 µg ml⁻¹); Dx: electroporated with the *McDx* siRNA (0.4 and 0.8 µg ml⁻¹). (C) The cumulative number of post-larvae at each time point of the metamorphosis assay (EPI induction) in control and *McDy* siRNA, non-sense siRNA electroporated pediveliger larvae. The results are presented as the mean ± SEM of nine experimental replicates (each containing 20 individuals). (D) Viability of mussel larvae in the metamorphosis assay (EPI induction) after electroporation with *McDy* siRNA or non-sense siRNA.

in the pediveliger larvae (**Figure 1D**). Serotonin (5-HT) and FMRFamide are neuronal markers for identifying the ganglia and developing the nervous system in molluscs (Voronezhskaya et al., 2002; Voronezhskaya et al., 2008; Yurchenko et al., 2018). The 5-HT and FMRFamide immunoreactivities showed some overlapping areas with stripe-like *McDx* signal as shown by WISH in the pediveliger larvae, especially for 5-HT-*lir* neurons (**Figures 1D, 2**), which suggests that *McDx* might be involved in neuronal development. These results are in line with a vertebrate study showing that D2 was extensively expressed in the embryonic brain prior to metamorphosis, which correlates closely with the developing neuron system in *X. laevis* (Cai and Brown, 2004). Serotonin has been reported to mediate the ciliary-based swimming activity of the mussel *M. edulis* larvae (Beiras and Widdows, 1995), and the 5-HT immunoreactivities were found in the velum position of the pediveliger larvae (**Figures 2C, D, S3B**). The expression of *McDy* in the velum may correlate closely with the motor and feeding functions in the pediveliger larvae (**Figure 1H**).

Larval metamorphosis is a complex process in which many neuroendocrine pathways are mediated. Although many other pathways participate in bivalve larval metamorphosis, such as dopaminergic, serotonergic, and cholinergic pathways (Joyce and Vogeler, 2018), the adrenergic signalling pathway is a classical neuroendocrine pathway that triggers metamorphosis in many bivalve species, including *M. coruscus* (Bonar et al., 1990; Garcia-Lavandeira et al., 2005; Yang et al., 2014; Di et al., 2020). In vertebrates, the adrenergic pathway is able to stimulate the THs system by activating deiodinases (Silva and Bianco, 2008) which supports the notion that a synergistic action between the adrenergic signalling pathway and the THs system occurs.

Our previous study revealed that knockdown effects of *McTR* using siRNA significantly reduced larval metamorphosis in *M. coruscus*, and suggested crosstalk between adrenergic signalling and the THs system (Li et al., 2020). The present study employed the siRNA transfection approach as previously reported and demonstrated that the knockdown effects of *McDx* and *McDy* the metamorphosis inducing activity (% post-larvae) of EPI was significantly lower (**Figures 3, 4**). It corroborates our previous findings that knockdown effects of *McDx* and *McDy* siRNA transfection might interfere with the “competence” of pediveliger larvae metamorphic transformation by inhibiting the ability of larvae in response to the inducer. Another important observation was that *McTR* siRNA knockdown not only inhibited metamorphosis but also reduced larval viability in *M. coruscus* (Li et al., 2020). However, the reduction in larval metamorphosis caused by siRNA knockdown of *McDx* and *McDy* did not associate with larval viability (**Figures 3D, 4D**). It may indicate that the knockdown effects of *McDx* and *McDy* repress metamorphic induction rather than larval viability, which does not elicit a lethal effect. These findings are consistent with our previous research that reported THs synthesis and metabolism inhibitor compounds MMI and PTU dramatically inhibited EPI-induced larval metamorphosis in *M. coruscus* (Li et al., 2021). In addition, the expression of *McDx* and *McDy* is not always equal

to the activity of deiodinase proteins. More studies are required to explore the role of *McDx* and *McDy* in larval metamorphosis.

In conclusion, the expression data strongly suggest that *McDx* and *McDy* contribute to developing visceral tissues, nervous system, mantle and velum (locomotory organ), indicating that two deiodinase genes play an important role during larval development in *M. coruscus*. The *McDx* and *McDy* knockdown significantly inhibited *McDx* and *McDy* gene expression and a significant reduction in EPI-induced larval metamorphosis. While this inhibition effect of *McDx* and *McDy* does not correlate with a reduction of larval viability as previously described in *McTR* knockdown experiments (Li et al., 2020). It is hypothesised that the knockdown effects of *McDx* and *McDy* repress metamorphic induction rather than larval viability, which does not elicit a lethal effect. Future investigations regarding the relationship between the adrenergic signalling pathway and the THs system will lead us to understand the evolution of the THs system and also their effects on larval development and metamorphosis.

DATA AVAILABILITY STATEMENT

The datasets presented in this study can be found in online repositories. The names of the repository/repositories and accession number(s) can be found in the article/**Supplementary Material**.

ETHICS STATEMENT

The experimental tests and animal handling procedures performed in this study were approved by the Institutional Animal Care and Use Committee (IACUC) of Shanghai Ocean University with the registration number of SHOU-DW-2018-013.

AUTHOR CONTRIBUTIONS

Y-FL designed the experiments. XS, Y-QW and Y-MY performed the experiments. Y-FL, XS and Y-QW analyzed the data. Y-FL and XS critically reviewed the data and wrote the manuscript. All authors read and approved the manuscript.

FUNDING

This study was supported by the National Natural Science Foundation of China (No. 31802321) and Science and technology innovation action plan (19590750500).

SUPPLEMENTARY MATERIAL

The Supplementary Material for this article can be found online at: <https://www.frontiersin.org/articles/10.3389/fmars.2022.914283/full#supplementary-material>

REFERENCES

- Beiras, R. and Widdows, J. (1995). Effect of the Neurotransmitters Dopamine, Derotonin and Norepinephrine on the Ciliary Activity of Mussel (*Mytilus Edulis*) Larvae. *Mar. Biol.* 122, 597–603. doi: 10.1007/BF00350681
- Bonar, D. B., Coon, S. L., Walch, M., Weiner, R. M. and Fitt, W. (1990). Control of Oyster Settlement and Metamorphosis by Endogenous and Exogenous Chemical Cues. *B. Mar. Sci.* 46 (2), 484–498. doi: 10.1515/botm.1990.33.2.219
- Burke, R. D. (1983). The Induction of Metamorphosis of Marine Invertebrate Larvae: Stimulus and Response. *Can. J. Zool.* 61, 1701–1719. doi: 10.1139/z83-221
- Cai, L. and Brown, D. D. (2004). Expression of Type II Iodothyronine Deiodinase Marks the Time That a Tissue Responds to Thyroid Hormone-Induced Metamorphosis in *Xenopus Laevis*. *Dev. Biol.* 266 (1), 87–95. doi: 10.1016/j.ydbio.2003.10.005
- Campinho, M. A., Galay-Burgos, M., Silva, N., Costa, R. A., Alves, R. N., Sweeney, G. E., et al. (2012). Molecular and Cellular Changes in Skin and Muscle During Metamorphosis of Atlantic Halibut (*Hippoglossus Hippoglossus*) are Accompanied by Changes in Deiodinases Expression. *Cell. Tissue. Res.* 350 (2), 333–346. doi: 10.1007/s00441-012-1473-x
- Campinho, M. A., Galay-Burgos, M., Sweeney, G. E. and Power, D. M. (2010). Coordination of Deiodinase and Thyroid Hormone Receptor Expression During the Larval to Juvenile Transition in Sea Bream (*Sparus Aurata*, *Linnaeus*). *Gen. Comp. Endocrinol.* 165 (2), 181–194. doi: 10.1016/j.ygcen.2009.06.020
- Campinho, M. A., Silva, N., Martins, G., Anjos, L., Florindo, C., Román-Padilla, J., et al. (2018). A Thyroid Hormone Regulated Asymmetric Responsive Centre is Correlated With Eye Migration During Flatfish Metamorphosis. *Sci. Rep.* 8 (1), 12267. doi: 10.1038/s41598-018-29957-8
- Carlsson, G. and Norrgren, L. (2007). The Impact of the Goitrogen 6-Propylthiouracil (PTU) on West-African Clawed Frog (*Xenopus Tropicalis*) Exposed During Metamorphosis. *Aquat. Toxicol.* 82 (1), 55–62. doi: 10.1016/j.aquatox.2007.01.005
- Darras, V. M. and Van Herck, S. L. (2012). Iodothyronine Deiodinase Structure and Function: From Ascidians to Humans. *J. Endocrinol.* 215 (2), 189–206. doi: 10.1530/joe-12-0204
- Di, G., Xiao, X. H., Tong, M. H., Chen, X. H., Li, L., Huang, M. Q., et al. (2020). Proteome of Larval Metamorphosis Induced by Epinephrine in the Fujian Oyster *Crassostrea Angulata*. *BMC Genomics* 21 (1), 675. doi: 10.1186/s12864-020-07066-z
- Garcia-Lavandeira, M., Silva, A., Abad, M., Pazos, A. J., Sanchez, J. L. and Perez-Paralle, M. L. (2005). Effects of GABA and Epinephrine on the Settlement and Metamorphosis of the Larvae of Four Species of Bivalve Molluscs. *J. Exp. Mar. Biol. Ecol.* 316 (2), 149–156. doi: 10.1016/j.jembe.2004.10.011
- Hadfield, M. (2000). Why and How Marine-Invertebrate Larvae Metamorphose So Fast. *Semin. Cell. Mar. Biol.* 11 (6), 437–443. doi: 10.1006/scdb.2000.0197
- Hadfield, M. G. (2011). Biofilms and Marine Invertebrate Larvae: What Bacteria Produce That Larvae Use to Choose Settlement Sites. *Annu. Rev. Mar. Sci.* 3, 453–470. doi: 10.1146/annurev-marine-120709-142753
- Huang, W., Xu, F., Qu, T., Li, L., Que, H. Y. and Zhang, G. F. (2015). Iodothyronine Deiodinase Gene Analysis of the Pacific Oyster *Crassostrea Gigas* Reveals Possible Conservation of Thyroid Hormone Feedback Regulation Mechanism in Mollusks. *Chin. J. Oceanol. Limn.* 33, 997–1006. doi: 10.1007/s00343-015-4300-x
- Huan, P., Wang, Q., Tan, S. J. and Liu, B. Z. (2020). Dorsoroventral Decoupling of Hox Gene Expression Underpins the Diversification of Molluscs. *Proc. Natl. Acad. Sci.* 117 (1), 503–512. doi: 10.1073/pnas.1907328117
- Joyce, A. and Vogeler, S. (2018). Molluscan Bivalve Settlement and Metamorphosis: Neuroendocrine Inducers and Morphogenetic Responses. *Aquaculture* 487, 64–82. doi: 10.1016/j.aquaculture.2018.01.002
- Laudet, V. (2011). The Origins and Evolution of Vertebrate Metamorphosis. *Curr. Biol.* 21 (18), R726–R737. doi: 10.1016/j.cub.2011.07.030
- Li, Y. F., Cheng, Y. L., Chen, K., Cheng, Z. Y., Zhu, X., Cardoso, J. C. R., et al. (2020). Thyroid Hormone Receptor: A New Player in Epinephrine-Induced Larval Metamorphosis of the Hard-Shelled Mussel. *Gen. Comp. Endocrinol.* 287, 113347. doi: 10.1016/j.ygcen.2019.113347
- Li, S. G., Liu, Y. J., Huang, J. L., Zhan, A. B., Xie, L. P. and Zhang, R. Q. (2017). The Receptor Genes *PjBMPRIb* and *PjBAMBI* are Involved in Regulating Shell Biomineralization in the Pearl Oyster *Pinctada Fucata*. *Sci. Rep.* 7, 9219. doi: 10.1038/s41598-017-10011-y
- Li, Y. F., Wang, Y. Q., Zheng, Y., Shi, X., Wang, C., Cheng, Y. L., et al. (2021). Larval Metamorphosis is Inhibited by Methimazole and Propylthiouracil That Reveals Possible Hormonal Action in the Mussel *Mytilus Coruscus*. *Sci. Rep.* 11, 19288. doi: 10.1038/s41598-021-98930-9
- Paris, M. and Laudet, V. (2008). The History of a Developmental Stage: Metamorphosis in Chordates. *Genesis* 46 (11), 657–672. doi: 10.1002/dvg.20443
- Power, D. M., Llewellyn, L., Faustino, M., Nowell, M. A., Björnsson, B. T., Einarsdottir, I. E., et al. (2001). Thyroid Hormones in Growth and Development of Fish. *Comp. Biochem. Physiol. C Toxicol. Pharmacol.* 130 (4), 447–459. doi: 10.1016/S1532-0456(01)00271-X
- Qian, P. Y. (1999). Larval Settlement of Polychaetes. *Hydrobiologia* 402, 239–253. doi: 10.1023/A:1003704928668
- Shepherdley, C. A., Klootwijk, W., Makabe, K. W., Visser, T. J. and Kuiper, G. G. (2004). An Ascidian Homolog of Vertebrate Iodothyronine Deiodinases. *Endocrinology* 145 (3), 1255–1268. doi: 10.1210/en.2003-1248
- Silva, J. E. and Bianco, S. D. (2008). Thyroid-Adrenergic Interactions: Physiological and Clinical Implications. *Thyroid* 18 (2), 157–165. doi: 10.1089/thy.2007.0252
- Strathmann, R. R. (1978). The Evolution and Loss of Feeding Larval Stages of Marine Invertebrates. *Evolution* 32 (4), 894–906. doi: 10.1111/j.1558-5646.1978.tb04642.x
- Thisse, C., Degraeve, A., Kryukov, G. V., Gladyshev, V. N., Obrecht-Pflumio, S., Krol, A., et al. (2003). Spatial and Temporal Expression Patterns of Selenoprotein Genes During Embryogenesis in Zebrafish. *Gene Expr. Patterns* 3 (4), 525–532. doi: 10.1016/S1567-133X(03)00054-1
- Voronezhskaya, E. E., Nezhlin, L. P., Odintsova, N. A., Plummer, J. T. and Croll, R. P. (2008). Neuronal Development in Larval Mussel *Mytilus Trossulus* (Mollusca: Bivalvia). *Zoomorphology* 127, 97–110. doi: 10.1007/s00435-007-0055-z
- Voronezhskaya, E. E., Tyurin, S. A. and Nezhlin, L. P. (2002). Neuronal Development in Larval Chiton *Ischnochiton Hakodadensis* (Mollusca: Polyplacophora). *J. Comp. Neurol.* 444 (1), 25–38. doi: 10.1002/cne.10130
- Yang, J. L., Li, W. S., Liang, X., Li, Y. F., Chen, Y. R., Bao, W. Y., et al. (2014). Effects of Adrenoceptor Compounds on Larval Metamorphosis of the Mussel *Mytilus Coruscus*. *Aquaculture* 426–427, 282–287. doi: 10.1016/j.aquaculture.2014.02.019
- Yurchenko, O. V., Skiteva, O. I., Voronezhskaya, E. E. and Dyachuk, V. A. (2018). Nervous System Development in the Pacific Oyster, *Crassostrea Gigas* (Mollusca: Bivalvia). *Front. Zool.* 15, 10. doi: 10.1186/s12983-018-0259-8

Conflict of Interest: The authors declare that the research was conducted in the absence of any commercial or financial relationships that could be construed as a potential conflict of interest.

Publisher's Note: All claims expressed in this article are solely those of the authors and do not necessarily represent those of their affiliated organizations, or those of the publisher, the editors and the reviewers. Any product that may be evaluated in this article, or claim that may be made by its manufacturer, is not guaranteed or endorsed by the publisher.

Copyright © 2022 Shi, Wang, Yang and Li. This is an open-access article distributed under the terms of the Creative Commons Attribution License (CC BY). The use, distribution or reproduction in other forums is permitted, provided the original author(s) and the copyright owner(s) are credited and that the original publication in this journal is cited, in accordance with accepted academic practice. No use, distribution or reproduction is permitted which does not comply with these terms.